Journal of Materials Chemistry A

PAPER

Cite this: *J. Mater. Chem. A*, 2015, **3**, 4435

Double-layered reactive microcapsules with excellent thermal and non-polar solvent resistance for self-healing coatings

Dawei Sun, Jinliang An, Gang Wu and Jinglei Yang*

Received 7th October 2014
Accepted 5th January 2015

DOI: 10.1039/c4ta05339g

www.rsc.org/MaterialsA

Double-layered polyurea microcapsules containing hexamethylene diisocyanate (HDI) with outstanding shell tightness have been successfully synthesized *via* interfacial polymerization reaction in an oil-in-water emulsion. The resultant capsules were systematically characterized by scanning electron microscopy (SEM), thermogravimetric analysis (TGA) and Fourier transform infrared (FTIR) spectroscopy. The reaction parameters including reaction temperature (40 °C, 50 °C, 60 °C), reaction duration (1 h, 1.5 h, 2 h and 2.5 h), amount of Suprasec 2644 (2.4 g, 3 g and 3.6 g) and emulsification time (15 min, 45 min and 75 min) were investigated and evaluated in terms of core fraction and quality of microcapsules. The core fraction of microcapsules was reduced with an increase of reaction temperature, reaction duration, mass of Suprasec 2644 and emulsification time, while the quality of microcapsules fluctuated. The thermal and organic solvent resistances were assessed by using TGA and titration. The results showed that the microcapsules had 1.6% weight loss compared with pure HDI with 90% weight loss after 60 min isothermal treatment at 100 °C. After immersion in various solvents for 24 days, the microcapsules released as low as ~3% of core in weakly polar solvents (*i.e.* hexane and xylene), about 5–60% in polar aprotic solvents (*i.e.* ethyl acetate, acetone, DMF and DMSO), and 60–90% in water and polar protic solvents (*i.e.* isopropanol and ethylene glycol). Both fresh and hexane-treated HDI capsules showed excellent anticorrosion performance in scratched coatings *via* self-healing functionality, indicating promising practical application in industrial coating and paint systems.

1. Introduction

Corrosion is a worldwide issue and involves very large economic expense for its prevention. Protective coatings as the most convenient method are one of the major approaches applied for corrosion protection. However, protective coatings as the outermost layer of structures are always at risk of damage during transportation, installation, and service, which could cause an absence of their barrier performance, and tremendous economic and life losses[1] due to many undetectable microcracks. Therefore, there is a great requirement for new-generation protective coatings that can intelligently respond to damage and recover functionality automatically to retard corrosion of metal substrates.

Self-healing materials have drawn great attention in the last decade[2–5] due to the ability to heal damage automatically wherever and whenever it occurs in the material. The self-healing function of materials can be achieved *via* embedding various containers such as capsules,[6–12] hollow fibers[13–15] or vasculature systems[16–19] into a matrix, or reconstructing intrinsic dynamic chemical bonds in the molecular structures of materials.[20,21] However, the complex manufacturing process of hollow fiber[11] and vasculature systems[22] and the limited ability to heal large cracks with bond reconstruction[23] restrict their applications in self-healing materials. Alternatively, encapsulation of various reactive chemicals in microcapsules has been reported widely as one of the most important approaches to obtain self-healing materials, especially self-healing coatings. Up to now, dicyclopentadiene,[7,24] amine,[25] and epoxy[26] have been microencapsulated successfully for self-healing materials. In order to avoid the contamination of catalyst, a dual microcapsule system was developed.[8] However, for satisfactory self-healing performance, an accurate stoichiometric ratio of the reactants at the site of damage is required, which restricts the practical applications of the above self-healing systems based on a two-component healing mechanism. A one-component, catalyst-free self-healing system as a more promising candidate for practical applications has been developed. Typically, liquid diisocyanates such as isophorone diisocyanate[27] and hexamethylene diisocyanate (HDI)[28] were efficiently microencapsulated and successfully applied to self-healing anticorrosion coatings.[29]

Owing to their easy modifiability, polymers are widely used to produce various protective coatings. However, in commercial coatings or paints, aqueous and organic solvents are widely

School of Mechanical and Aerospace Engineering, Nanyang Technological University, Singapore 639798. E-mail: mjlyang@ntu.edu.sg; Tel: +65 67906906

used to lower resin viscosity for easy processing or economic purposes. In addition, a heat treatment at elevated temperature is widely implemented to remove solvent retention or cure coating matrix for higher T_g and better chemical resistance. Therefore, appropriate solvent, water and thermal resistances for microcapsules used for self-healing anticorrosion application in practical coatings or paints must be highlighted. Although excellent self-healing anticorrosion performance for microcapsule-embedded epoxy coatings without using water and any organic solvent has been reported, it is debatable for assessment in practical commercial coatings due to the poor resistances of these microcapsules in water[27,28] and organic solvents.[30]

A variety of approaches have been implemented to improve resistances of microcapsules. Fan and Zhou[31] improved the thermal resistance of microcapsules by dispersing layered silicate within the walls of the microcapsules. Tatiya *et al.*[32] applied dendritic functional monomer to improve thermal resistance of microcapsules by increasing the crosslink density of the shell. Yuan *et al.*[33] prepared poly(urea-formaldehyde) microcapsules containing epoxy resins and investigated related permeability and stability of the obtained microcapsules in thermal and solvent surroundings. Wu *et al.*[34] synthesized silica/polyurea hybrid microcapsules loaded with HDI as core materials which showed obvious improvement in xylene resistance. Furthermore, Wu *et al.*[35] encapsulated various liquid reactive reagents with poly(urea-formaldehyde) which showed superior solvent and heat resistances.

In this study, we successfully fabricated HDI-filled double-walled polyurea microcapsules with excellent resistance to thermal environment and non-polar organic solvents. Self-healing coatings mixed with fresh and hexane-treated microcapsules were prepared to assess the anticorrosion performance under an accelerated corrosion process.

2. Experimental

2.1 Materials

4,4′-Diphenylmethane diisocyanate (MDI) prepolymer (Suprasec 2644) was obtained from Huntsman. HDI, gum arabic, triethylenetetramine (TETA), hydrochloric acid solution (HCl, 0.1 M), potassium bromide (KBr), sodium hydroxide (NaOH), sodium chloride (NaCl), dimethylsulfoxide (DMSO), dimethylformamide (DMF), acetone, ethyl acetate, xylene, hexane, ethylene glycol and isopropanol were purchased from Sigma-Aldrich. Epolam 5015 and hardener 5015 used as epoxy matrix were supplied by Axson. All the chemicals in this study were used as received without further purification.

2.2 Synthesis of polyurea microcapsules containing HDI

The microcapsules containing HDI were synthesized *via* interfacial polymerization in an oil-in-water emulsion. Firstly, the oil phase, 3.0 g of Suprasec 2644 and 13.5 g of HDI, was prepared by mixing at 70 °C on a programmable hotplate. The water phase, 90 ml of deionized (DI) water with 2.5 wt% gum arabic as surfactant, was heated up to 50 °C in a 1000 ml beaker at an agitation rate of 550 rpm (Caframo, model: BDC6015). The beaker was placed in a temperature-controlled water bath located on a programmable hotplate. Later, the oil phase was poured into the water solution under agitation for emulsification. After the emulsion system was stabilized for 45 min, 0.8 wt% TETA aqueous solution was added dropwise into the system to initiate the interfacial polymerization. In order to control the reaction process, 90 ml TETA solution in total was added equally into the mixture in 12 portions at intervals of about 5 min. After that, the system further reacted for another 2 h. The obtained suspension of microcapsule slurry was rinsed with DI water 3–4 times. Finally, the collected microcapsules were air-dried for 6 h and then sieved to remove debris for further analysis.

2.3 Characterization of HDI-filled microcapsules

The size, morphology, and shell thickness of the obtained microcapsules were observed using a scanning electron microscope (SEM, JOEL JSM 5600LV). The size distributions of the microcapsules were measured from the SEM images using ImageJ based on at least 150 individuals. Microcapsules were mounted on conductive tape and some of them were ruptured with a razor blade to observe the cross-section.

A spectrophotometer (Varian 3100) was applied to obtain FTIR spectra of pure HDI, Suprasec 2644, pure capsule shell, capsule core material and full capsules mixed with KBr pellets separately in order to identify the composition.

2.4 Thermal stability and core fraction

The thermal property and composition of microcapsules were characterized using thermogravimetric analysis (TGA, Hi-Res Modulated TGA 2950). In all the TGA tests, 10–20 mg powder samples were placed in a platinum pan and heated under nitrogen atmosphere at a heating rate of 10 °C min^{-1}.

To calculate the core fraction of the synthesized microcapsules, powder samples were heated to 160 °C and stabilized for 1 hour until no weight change, meaning total evaporation of HDI inside. Then the sample was further heated to 600 °C for complete decomposition. The difference between residue weight at the initial temperature and that remaining at 160 °C was equal to the core fraction of the microcapsules.

To evaluate the thermal stability of the microcapsules, the weight loss during an isothermal process at 100 °C for 60 min under nitrogen atmosphere was measured.

2.5 Release behavior of capsule core in solvents

2.5.1 In non-polar solvents and polar aprotic solvents. Non-polar solvents including hexane and xylene and polar aprotic solvents including ethyl acetate, acetone, DMF and DMSO were considered in this investigation. All the organic solvents were anhydrous to avoid the influence of residual water on the measurements. All the processes were carried out in a dry oven to minimize the influence of the moisture in the surroundings. At room temperature, 1.5 ml solvent with 10 wt% microcapsules was well sealed in a 20 ml vial. After a certain duration, 1 ml of organic solvent was extracted quickly with a

plastic dropper into a beaker. The released HDI in organic solvent could be titrated according to ASTM Standard D2572-97. Eventually, the relative released percentage of the core material can be calculated simply as follows:

$$\mathrm{NCO\%} = \frac{(V_{\mathrm{blank}} - V) \times C_{(\mathrm{HCl})} \times 0.042}{m_{\mathrm{sample}}} \times 100\% \quad (1)$$

$$m_{(\mathrm{HDI\ release})} = 2 \times m_{\mathrm{solvent}} \times \frac{\mathrm{NCO\%}}{1 - 2\mathrm{NCO\%}} \quad (2)$$

$$\mathrm{HDI_{release}\ wt\%} = \frac{m_{(\mathrm{HDI\ release})}}{m_{(\mathrm{HDI\ encapsulated})}} \times 100\% \quad (3)$$

where NCO% is the NCO content in organic solvent and $\mathrm{HDI_{release}}$ wt% is the percentage of HDI released from microcapsules. V_{blank} (ml) and V (ml) are the volumes of the standard HCl (0.1 M) aqueous solution consumed by the blank experiment and titration sample, respectively. $C_{(\mathrm{HCl})}$ is the normality of standard HCl (0.1 M) aqueous solution, 0.042 is the milliequivalent weight of the NCO group, and m_{sample} (g), $m_{(\mathrm{HDI\ released})}$ (g), m_{solvent} (g) and $m_{(\mathrm{HDI\ encapsulated})}$ (g) are the masses of sample, total HDI in solvent, solvent and encapsulated HDI in the initial microcapsules, respectively.

2.5.2 In polar protic solvents. Polar protic solvents including water, ethylene glycol and isopropanol were used to immerse microcapsules with 10 wt% concentration. TGA instead of titration was applied to monitor the variation of core fraction with the increase of immersion time in polar protic solvents due to the reactivity of isocyanate with hydroxyl of the solvent molecules.

2.6 Preparation of self-healing anticorrosion coating

The prepared microcapsules were initially mixed into epoxy resin (EPolam 5015, AXSON) to 10 wt% at ambient temperature, followed by addition of hexane (5 wt%) as thinner. Several pieces of steel panel ($50 \times 50 \times 2\ \mathrm{mm^3}$) were polished with sand paper, then degreased with acetone, and finally washed with distilled water. Afterwards, each dried panel was coated with the self-healing coating to a final thickness of 600 μm. The coating was firstly cured at room temperature for 24 h. After 24 h, scratches were applied manually on the coating by a razor blade. Control coating with pure epoxy was prepared with the same procedure. Both the self-healing and control samples were immersed in 10 wt% of NaCl solution for 24 h to evaluate their corrosion performance.

3. Results and discussion

3.1 Formation mechanism of double-layered capsule shell

Double-layered capsule shell was formed *via* interfacial polymerization in the emulsion as shown in Fig. 1a–c. Firstly, the mixture of Suprasec 2644 and HDI was dispersed in gum arabic aqueous solution to generate a stable oil-in-water emulsion within 15 min as shown in Fig. 1a. With an increase of emulsification time to 45 min, a very thin outer layer of microcapsule was formed gradually from the polymerization of Suprasec 2644 and chemicals with activated hydrogen (–OH or $-NH_2$), as shown in Fig. 1b. Afterwards, the diluted TETA solution was introduced into the emulsion, and the TETA molecules diffused gradually inwards across the outer layer of the microcapsules to form an inner layer after reacting with Suprasec 2644.

To further verify this process, additional investigations were carried out. After emulsification for 15 min, the micro-droplets were covered by a very thin membrane (Fig. $1a_1$), which was dissolvable in acetone, meaning a very short oligomer in this layer was forming and growing during this emulsification time. With an increase of emulsification time to 45 min, the oligomer on the surface of micro-droplets reacted with surfactant and/or water that have active functional groups to slowly form a smooth and thin outer shell at the oil/water interface. The microcapsules with flexible outer shells are shown in Fig. $1b_1$. Gum arabic is a complex mixture of glycoproteins and polysaccharides. Glycoprotein as a kind of protein containing amino functional groups that is reactive to isocyanates.[36] Therefore, it is reasonable to consider that the outer shell is partially formed from the reaction between gum arabic and Suprasec 2644.

In addition, the microcapsules after emulsification for 45 min were immersed in and washed with acetone several times, and the profile of a crushed shell is shown in Fig. $1b_2$. It is observed that a layer of solid shell has been formed. The structure of the washed shell is very loose since the newly formed shell cannot resist the swelling of acetone leading to an increase of shell volume.[37] In addition, many solid aggregates in the interior of the microcapsules were observed. These particles were mainly attributed to the reaction between water and Suprasec 2644. From the beginning of the emulsification process, water molecules are able to diffuse gradually into micro-droplets, and prefer reacting with Suprasec 2644[28] to form solid particles due to the higher reactivity of MDI than HDI. The reason why water molecules can be dissolved in oil phase is that Suprasec 2644 contains many urethane bonds, which can absorb water through hydrogen bonding.[38] The outer membrane shell has poor stiffness for collection. After emulsification, diluted TETA solution was added to the emulsion system, and TETA molecules in the aqueous solution began to diffuse gradually across the outer layer to react with NCO groups due to their solubility in the formed polymer film.[39] With the product of polyurea, the shell started to thicken towards the organic phase. Finally, a mixture of polyurea with different crosslink density in the shell wall was formed from the abovementioned reactions together with some side reactions between NCO groups of prepolymer, HDI or intermediate polyisocyanates and hydroxyl groups of gum arabic or water.

3.2 Morphology of the resultant microcapsules

Spherical microcapsules are shown in Fig. 2a. Microcapsules with average diameter of 88 ± 22 μm were synthesized at an agitation rate of 550 rpm. It can be seen that the outer layer (Fig. 2b) of the microcapsules is quite smooth and dense due to slow reaction rate[40] and high crosslink density, while the inner shell is rough and loose due to the rapid reaction between TETA and isocyanates. The overall shell thickness of a microcapsule is

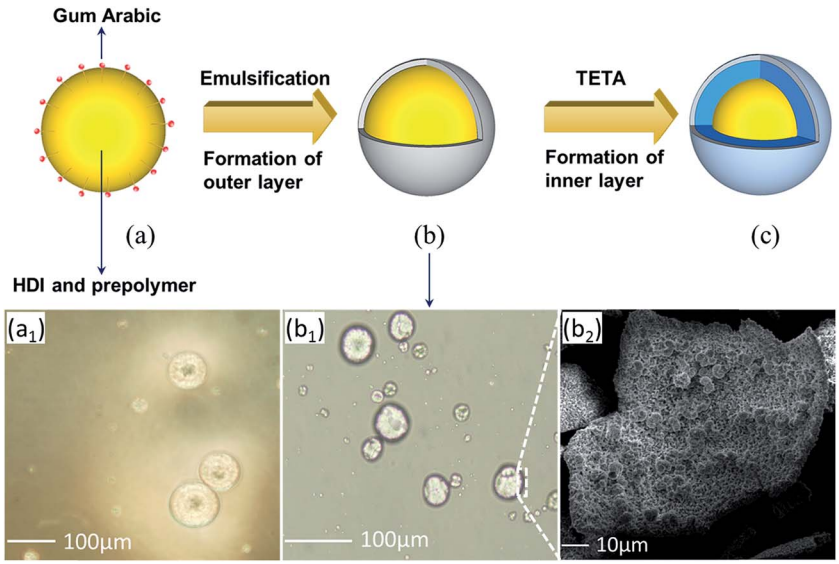

Fig. 1 Schematic formation process of double-layered polyurea microcapsule (not to scale): (a) oil droplets suspension was obtained after emulsification for 15 min; (b) the outer layer of microcapsules was formed after emulsification for 45 min; and (c) the inner wall of microcapsules was formed after introduction of TETA solution. Optical microscopic images showing the oil droplets with oligomer membrane-like shell (a_1) after emulsification for 15 min and microcapsules with crosslinked thin shell (b_1) after emulsification for 45 min in solution and the crushed shell after washing and collection (b_2).

uniform at around 7–8 μm as seen in Fig. 2c, and the inset in Fig. 2c shows the thickness of the outer layer at around 400 nm. As shown in Fig. 2c and d, an obvious separation was observed between inner and outer shell, indicating the double-layered profile of the microcapsule shell. The separation could be attributed to two factors: (1) interpenetrating polymer networks were not formed between the outer and inner shell because it is difficult for HDI molecules to migrate into the outer shell; (2) the formed outer shell is very smooth without voids or pores to interlock with the solidified inner shell.

3.3 Determination of microcapsule components

In order to identify the compositions of the obtained microcapsules, FTIR tests of core material, shell material, Suprasec 2644, and pure HDI were performed and the spectra are provided in Fig. 3. The spectrum of core material was nearly identical to that of pure HDI, indicating that HDI was successfully encapsulated without Suprasec 2644. The main reason is that Suprasec 2644 was totally exhausted by the diffused water and TETA. However, in the spectrum of the shell, the absorption bands at 2260 cm^{-1} corresponding to NCO stretch characteristic could still be observed, implying that NCO functional groups in the shell were not exhausted completely

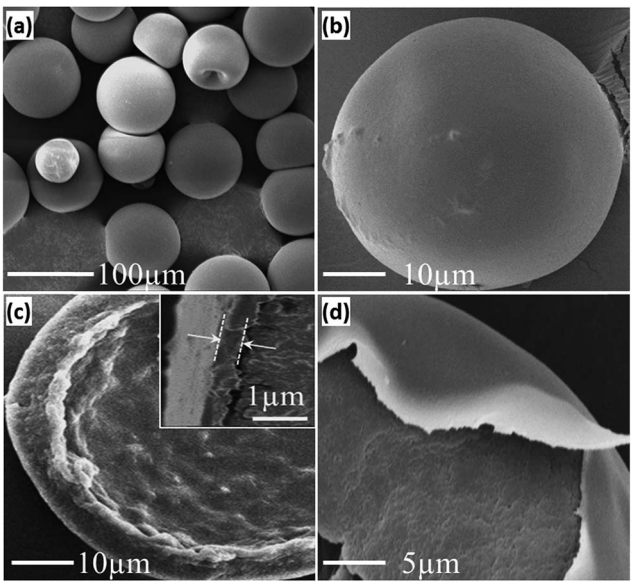

Fig. 2 Morphology of the synthesized microcapsules: (a) overview of spherical shaped microcapsules, (b) enlarged image of individual capsule showing smooth outer surface, (c) shell wall profile (inset: thin outer layer), and (d) double-layered structure of microcapsule shell.

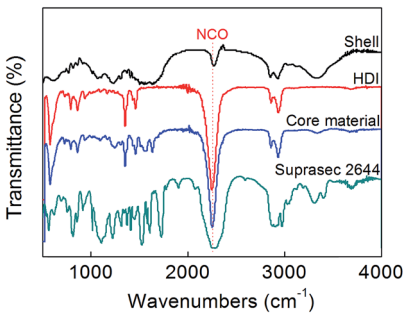

Fig. 3 Comparison of FTIR spectra of capsule's shell and core, Suprasec 2644 and HDI showing successful encapsulation of HDI as core material.

during the reaction process. This was because the formed shells with high crosslinking density restricted continuous consumption of residual NCO groups by the diffused water and TETA molecules.

3.4 Thermal property and core fraction of microcapsules

As shown in Fig. 4a, all materials including pure HDI, pure shell and microcapsules have no obvious weight loss at around 100 °C, meaning no water therein. In addition, pure HDI began to evaporate at 117 °C, and this process was completed at 160 °C. Pure shell began to decompose at around 250 °C and vanished at 600 °C. However, capsules began to lose weight at 148 °C, and their residual weight was 2.5 wt% at 600 °C, and the residue may be coke, which indicates that the encapsulated HDI had higher thermal stability than the pure HDI.

Fig. 4b shows that the residual weights of microcapsules and pure HDI vary with time during the isothermal process of 60 min at 100 °C. By comparison, pure HDI loses weight of approximately 90 wt% of original sample, and encapsulated HDI loses weight of around 1.6 wt% after the isothermal process. That means the encapsulated HDI had lower evaporation rate and further confirmed that resultant shells have better thermal resistance compared with pure HDI.

The core fraction of microcapsules was determined by the weight loss of microcapsules from the beginning of the experiment to 160 °C. As shown in Fig. 4a, the weight loss of microcapsules was approximately 53.2 wt% from beginning to 160 °C and then reached a relatively stable plateau until 200 °C. Comparing with the weight loss curve of pure HDI, it is reasonable to consider that this weight loss was the HDI evaporation in the core of the microcapsules and was not accompanied with a decomposition of the shell. Therefore, the core fraction of microcapsules was 53.2 wt%.

3.5 Parametric study to optimize the encapsulation process

In order to find the optimal microencapsulation process, various parameters, namely reaction temperature, reaction duration, mass of Suprasec 2644 and emulsification time, were studied and evaluated in terms of quality and core fraction of the resultant capsules.

3.5.1 Reaction temperature. Reaction temperatures of 40 °C, 50 °C and 60 °C were investigated and evaluated in terms of core fraction of microcapsules and thermal resistance. As shown in Fig. 5a, the core fraction of microcapsules decreased from 65.8 wt% to 53.2 wt% with increasing reaction temperature from 40 °C to 50 °C, and finally reached 0% when the reaction temperature was 60 °C. The decrease of core fraction was largely attributed to the side reaction between the diffused water and HDI in the core. Higher reaction temperature could accelerate the diffusion of water molecules into the microcapsules resulting in consumption of more HDI within the same reaction duration.

Moreover, before and after 60 min isothermal at 100 °C, the core fractions of microcapsules obtained at different reaction temperatures were compared. As shown in Fig. 5a, the core fraction was decreased from 65.8% to 32% when reaction temperature was 40 °C, while the core fraction decreased from 50.3% to 49.5% when reaction temperature was 50 °C. The smaller release of core material for the microcapsules prepared at higher reaction temperature reflected the denser shell structure. In addition, the temperature at which microcapsules lost 5% of their weight was increased from 103 °C to 145 °C with an increase of reaction temperature from 40 °C to 50 °C, supporting the improved thermal stability of the microcapsules.

3.5.2 Reaction duration. The influence of reaction durations of 1 h, 1.5 h, 2 h and 2.5 h on resultant microcapsules was investigated and evaluated in terms of core fraction and thermal resistance of microcapsules. As shown in Fig. 5b, the core fractions of original microcapsules decreased gradually from 59.6% to 42.9% when the reaction duration was extended from 1 h to 2.5 h. The increasing consumption of HDI by water or TETA with increasing reaction duration contributed to this result.

In addition, the core fraction of microcapsules decreased from 59.6% to 53.5% after 60 min isothermal at 100 °C when the reaction duration was 1 h, and the released HDI of microcapsules was around 6.1 wt%. The released amount of core material after the isothermal process decreased gradually with

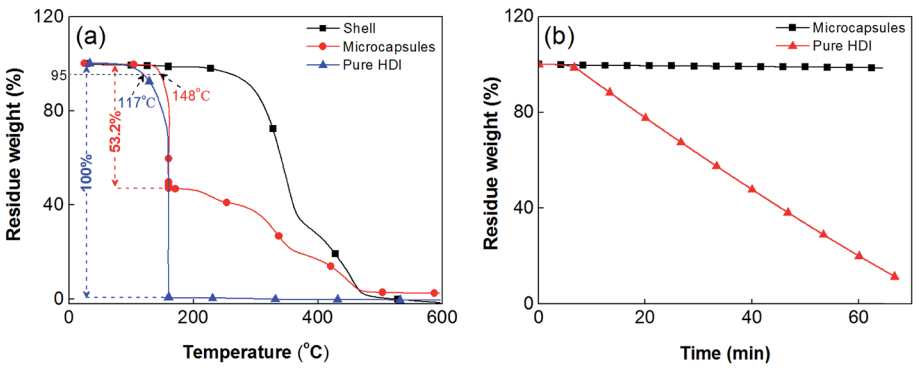

Fig. 4 Thermal performances of resultant microcapsules and constituent materials. (a) TGA curves of the resultant microcapsules, pure HDI and shell as a function of temperature at a heating rate of 10 °C min^{-1} in N_2 atmosphere. (b) TGA isothermal curves of the resultant microcapsules and pure HDI at 100 °C for 60 min in N_2 atmosphere.

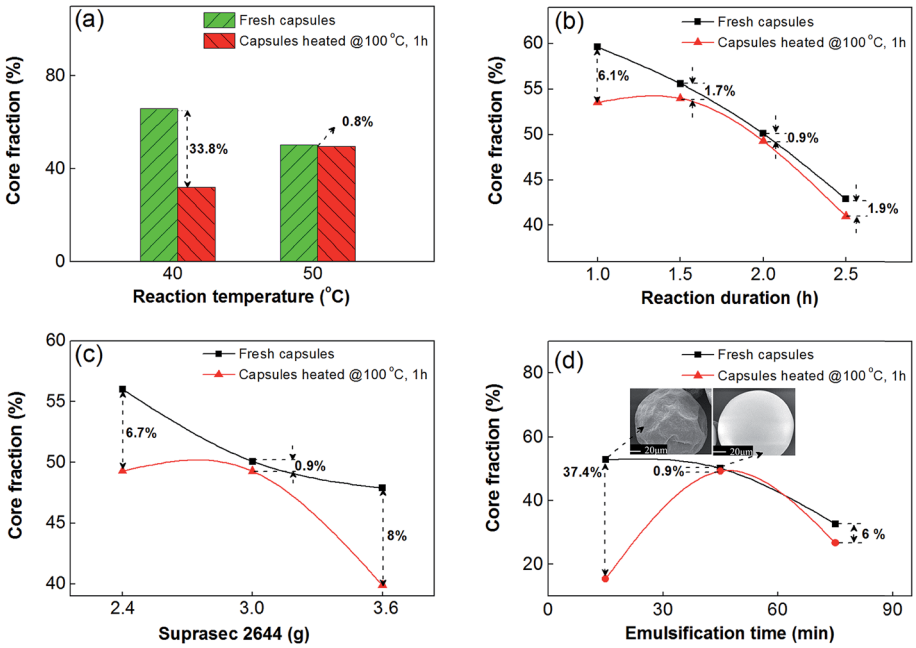

Fig. 5 Optimization of the encapsulation process evaluated by the core fraction of fresh synthesized and thermally treated microcapsules. The parameters investigated were: (a) reaction temperature, (b) reaction duration, (c) amount of Suprasec 2644, and (d) emulsification time.

increasing reaction duration, and reached a lowest value (0.9 wt%) when the reaction duration was 2 h. Subsequently, the released amount of core material after the isothermal process started to increase from 0.9 wt% to 1.9 wt% with increasing reaction duration to 2.5 h. This phenomenon indicates that the tightness of the microcapsule shell is first improved and then deteriorated with the extension of reaction duration. The improvement of tightness is probably because more NCO groups were cured, and thus a denser shell was produced at longer reaction duration. However, on continuing to prolong the reaction duration, the hydrolysis of the shell would impair the compactness of the shell and induce the release of core.[41] Another reason for the deterioration of shell compactness may be that more water molecules diffused into the core of the microcapsules and consumed more HDI with longer reaction duration. Meanwhile, consumption of more HDI can produce more carbon dioxide (CO_2), which could produce more cavities and lead to undesirable structure of the shell,[42] and thus inducing the release of core material eventually.

Considering the core fraction and the thermal barrier property of the obtained microcapsules, it is suggested that the optimal reaction duration is about 2 h for this system.

3.5.3 Amount of Suprasec 2644. The influence of the mass of Suprasec 2644 of 2.4 g, 3.0 g and 3.6 g on the resultant microcapsules was investigated and evaluated in terms of core fraction and thermal resistance of microcapsules. As shown in Fig. 5c, the core fraction of microcapsules decreased from 56% to 47.9% with an increase of the mass of Suprasec 2644 from 2.4 g to 3.6 g. This was mainly because emulsified droplets contained lower fraction of HDI when more Suprasec 2644 was added in the oil phase. And lower HDI fraction in emulsified droplets produced microcapsules containing less core material within the same reaction duration.

In addition, the core fraction of microcapsules was decreased by 6.3% (from 56% to 49.7%) after 60 min isothermal at 100 °C when 2.4 g of Suprasec 2644 was used. Afterwards, the released amount of core material after the thermal process decreased gradually with increasing mass of Suprasec 2644, and reached a lowest value (0.9%) when the added mass of Suprasec 2644 was 3.0 g. Subsequently, the release of core material increased gradually when the mass of Suprasec 2644 was increased to 3.6 g. The fluctuating trend is because the addition of more Suprasec 2644 could raise the phenyl content in the shell, which improved the stiffness and thermal resistance of shells.[43] However, when the added mass of Suprasec 2644 was beyond the optimal value, a reduction of crosslink density of shell would weaken the barrier property of microcapsules because Suprasec 2644 has lower NCO content than HDI.

3.5.4 Emulsification time. The influence of emulsification time of 15 min, 45 min and 75 min on the resultant microcapsules was investigated and evaluated in terms of core fraction and thermal resistance of microcapsules. As shown in Fig. 5d, the core fraction of fresh capsules decreased from 52.8% to 32.6% with an increase of emulsification time from 15 min to 75 min. The greater consumption of core material by water for a longer emulsification time contributes to this phenomenon.

In addition, the core fraction of microcapsules was decreased by 37.4% (from 52.8% to 15.4%) after 60 min isothermal at 100 °C when the emulsification time was 15 min. Afterwards, the release of core material after the thermal process decreased gradually, and reached a lowest point (0.9%) when the emulsification time was 45 min. Subsequently, the release of core materials increases gradually with an increase of emulsification from 45 min to 75 min. It can be seen from the inset pictures of Fig. 5d that the microcapsules obtained at longer emulsification time had smoother and denser shells. However, when the

emulsification time exceeds the optimal value, the hydrolysis of the outer layer induces the release of core material during the isothermal process. Moreover, more carbon dioxide can be produced when a longer emulsification time was applied, leading to more voids and undesirable shell structure, which can induce the release of HDI.

3.6 Solvent resistance study of microcapsules

The release percentage of core material as a function of immersion time is shown in Fig. 6. The released core material increased gradually with increasing immersion duration in solvents. After a certain duration the release process was stopped, and the relative released percentage of HDI reached a plateau, which means the osmotic pressure at both sides of the shell reached a balance. After immersion in different polar aprotic solvents for 12 h, the released HDI of the original HDI were 2.6 wt% in hexane, 3.2 wt% in xylene, 5.3 wt% in ethyl acetate, 12.5 wt% in acetone, 21 wt% in DMF and 60 wt% in DMSO, as shown in Fig. 6a. In comparison, the reduced core material of the original were 87 wt% in water, 85.4 wt% in ethylene glycol and 62.6 wt% in isopropanol after the same duration in different polar protic solvents, as shown in Fig. 6b.

Normally, thermosetting matrices swell through imbibition after being placed in an organic solvent[44] and the mesh size of the network increases accordingly with the swelling process.[45] The swelling ratio of a polymer increases gradually with an increase in the polarity of organic solvents.[46,47] Then the small solute molecules may diffuse across the swelling network according to free volume theory[48] until osmotic pressure balance. Therein, different mechanisms are applied depending on the properties of the solvents including non-polar or weakly polar organic solvents (Fig. 7a), polar aprotic organic solvents (Fig. 7b), polar protic organic solvents (Fig. 7c) and water (Fig. 7d).

The shells of microcapsules that are immersed in weakly polar solvents like hexane and toluene (Fig. $7a_1$) are hardly swollen (Fig. $7a_2$) and the mesh size of polyurea network remains almost unchanged, resulting in almost no release of HDI core (Fig. $7a_3$). With an increase in the polarity of aprotic solvent molecules (Fig. $7b_1$), a larger swelling ratio and thus mesh size (Fig. $7b_2$) of microcapsule shell induce the release of HDI core (Fig. $7b_3$). However, when microcapsules were immersed in polar protic solvents (Fig. $7c_1$), besides the very large release of HDI core (Fig. $7c_3$) resulting from severe swelling of the shell (Fig. $7c_2$), the hydroxyl groups in the protic solvent molecules can react with HDI,[49] producing new polyurethane aggregates distributing in external organic solvent, shell and core region.

It is difficult for water to swell polyurethane[50] due to incompatibility, but water molecules can still diffuse across the polyurea shell by interacting with H-bonds.[38] When microcapsules are immersed in water (Fig. $7d_1$), water molecules can diffuse inwards and react with the HDI core at the internal surface of the shell (Fig. $7d_2$) to grow new polyurea materials, which thickens the shell (Fig. $7d_3$), and the barrier property is improved accordingly with depletion of HDI.

The residual HDI core, if any, after immersion in water and various solvents remains active.

By comparison of release phenomenon in Fig. 6a, it is observed that the release of core material increases obviously with solvent polarity. The main reason is that a solvent with higher polarity is more inclined to dissolve polar segments of polyurea due to the similar compatibility principle.[47] Then, the bigger mesh size produced by swelling of the shell allowed the passage of more HDI.[51] Therefore, polyurea as a polar material can offer better resistance to weakly polar solvents[52] due to lower swelling ratio. The outstanding non-polar and weakly polar solvent resistance is attributed to the unique double-layered shell structure by comparing with the organic solvent resistance from another investigation,[34] in which a polyurea/silica hybrid shell was prepared with similar thickness of 8 μm.

In addition, microcapsules showed better resistance to polar aprotic solvents than polar protic solvents as evident by comparison of Fig. 6a and b. The increase of HDI loss in polar protic solvents mainly results from the fact that isocyanates are reactive with substances containing hydroxyl groups. After swelling, the diffused-in polar protic solvents can react with core materials and the diffused-out isocyanates can react with hydroxyl groups, which accelerates the consumption of core

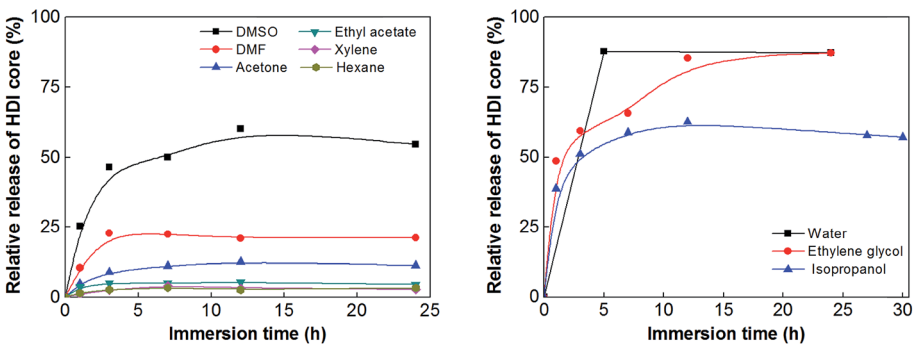

Fig. 6 Solvent resistance of the resultant microcapsules synthesized at the optimal conditions (*i.e.* emulsification time: 45 min; reaction temperature: 50 °C; reaction duration: 2 h; Suprasec 2644: 3 g). Relative release of core material over time after immersion of microcapsules in non-polar (hexane and xylene) and polar aprotic (ethylene acetate, acetone, DMF and DMSO) solvents (a) and in polar protic (isopropanol, ethylene glycol and water) solvents (b). The concentration of microcapsules in each solvent is 10 wt%.

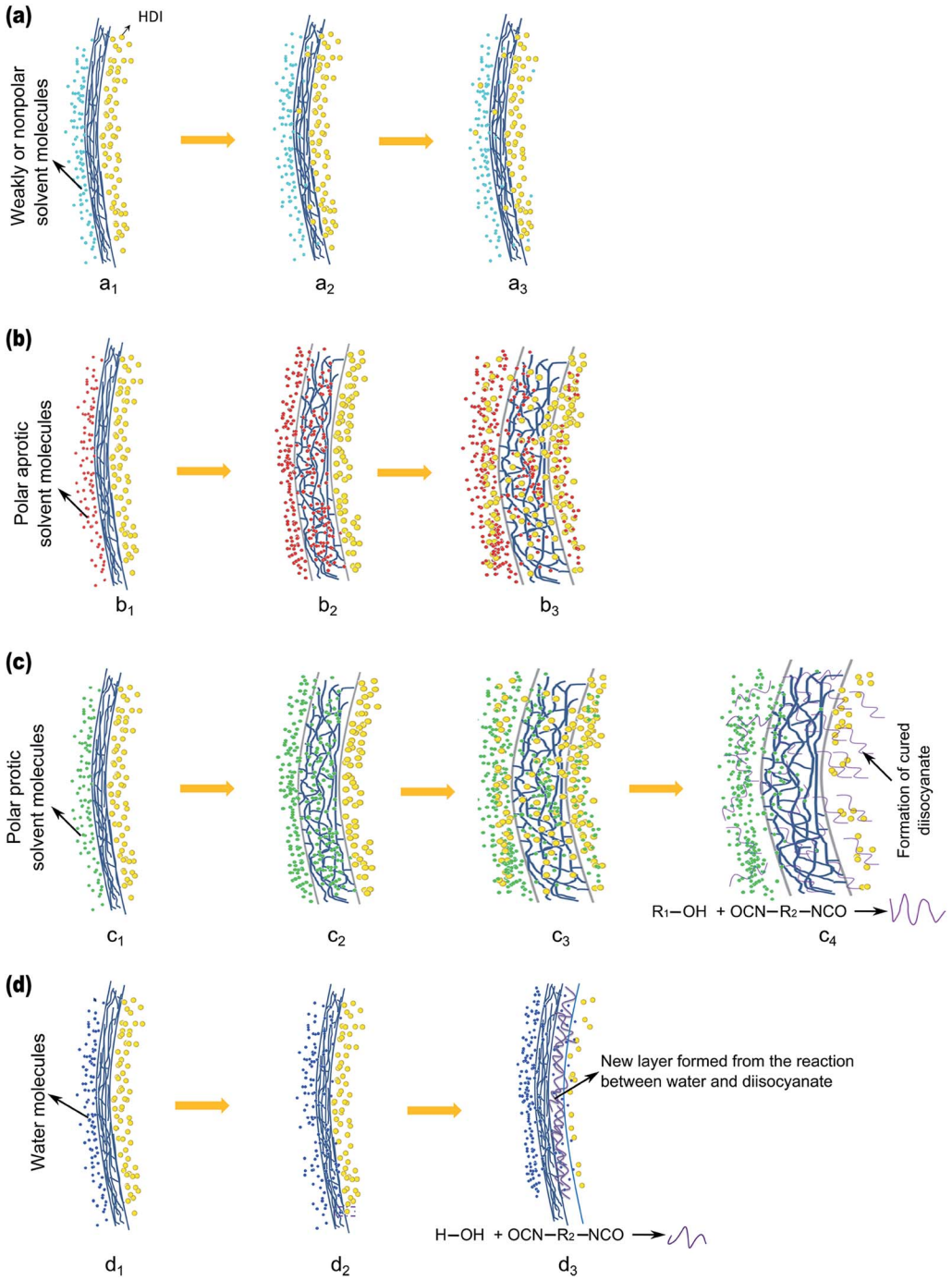

Fig. 7 Schematic diagrams showing different release mechanisms of core molecules through the shell after immersion in various types of solvents. (a) In weakly or non-polar solvents: initial state of immersion (a_1); slow diffusion of weakly polar solvent molecules resulting in marginal swelling of shell (a_2); balanced state with almost no release of HDI core in external solvents (a_3). (b) In polar aprotic solvents: initial state of immersion (b_1); easy diffusion of solvent molecules through shell and thus obvious swelling of shell (b_2); more HDI core diffusion out through swelling shell until balance (b_3). (c) In polar protic solvents: initial state of immersion (c_1); easy diffusion of solvent molecules through shell and thus obvious swelling of shell (c_2); severe loss of core material (c_3); formation of dispersed polyurethane aggregates from the reaction of HDI with hydroxyl groups in solvents (c_4). (d) In water: initial state of immersion (d_1); diffusion of water molecules into microcapsules without swelling effect (d_2); formation and growth of new polyurea layer on the internal surface of shell (d_3) until balance.

fraction with the product of new polyurethane materials distributing in external solvent, microcapsule shell and core region. Although microcapsule shells cannot be swollen by water molecules, these molecules can still diffuse into core part to react with HDI resulting in a decrease of core content.

From the above investigation, the resultant microcapsules have excellent resistance to non-polar solvents. The resistance gets worse gradually with an increase of solvent polarity. In polar protic solvents, the microcapsules show the poorest resistance.

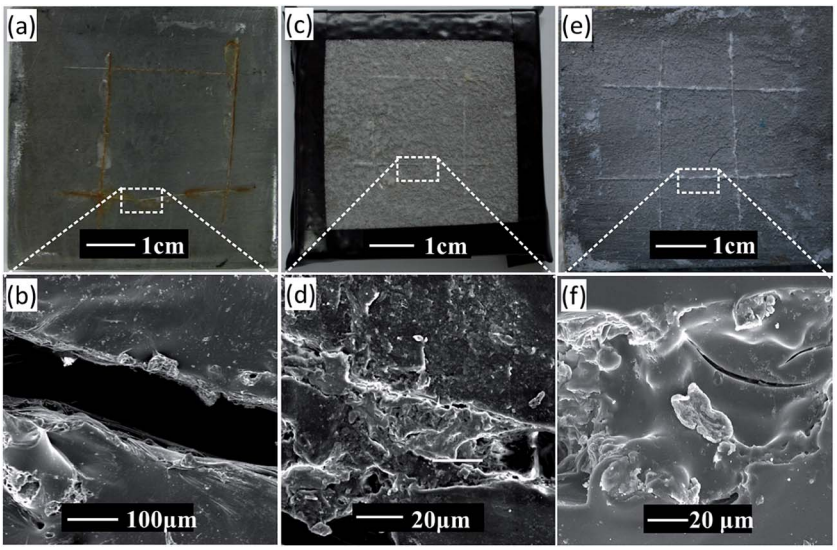

Fig. 8 Corrosion protection of steel panels coated with: (a) pure control epoxy coating, (c) self-healing epoxy coating prepared with 5 wt% hexane and 10 wt% of the resultant microcapsules, and (e) self-healing epoxy coating by incorporating 10 wt% microcapsules that were immersed in hexane for 30 days at 50 wt% concentration, after immersion in 10 wt% NaCl solution for 24 h. The fresh microcapsules were synthesized at the optimal conditions (*i.e.* emulsification time: 45 min; reaction temperature: 50 °C; reaction duration: 2 h; Suprasec 2644: 3 g). Micrographs of the scratched areas of (b) control coating, (d) self-healing coating with fresh microcapsules, and (f) self-healing coating with treated microcapsules after corrosion test.

3.7 Anticorrosion study

An industrial epoxy resin (Epolam 5015) was thinned by 5 wt% hexane to simulate a solvent-based coating, in which the fresh microcapsules were dispersed in epoxy resin at 10 wt% to prepare a self-healing coating. It is clearly shown in Fig. 8a that severe corrosion is observed in the control coating after 24 h immersion in a 10 wt% salt solution with a clear cut through the coating to the metal substrate. In comparison, as shown in Fig. 8c, it is seen that the scratched area of the steel panel coated with self-healing coating is nearly fully free of corrosion after salt water immersion with the sealed scratch (Fig. 8d) and very limited corroded region on the metal substrate. The released HDI from the ruptured microcapsules can seal and heal the crack automatically by reacting with surrounding moisture. The newly formed material was in this way able to retard corrosion of the steel panel. The result clearly demonstrates the efficient corrosion protection of self-healing coating over the steel panel.

In addition, the microcapsules immersed in hexane with a concentration of 50 wt% for 30 days were dispersed into epoxy resin at 10 wt% to prepare self-healing coating, where good anticorrosion performance is also observed similarly to that of the self-healing coating with fresh microcapsules, as shown in Fig. 8e. Newly formed material is observed in Fig. 8f as well, showing the functional reactive core remained even after harsh environmental treatment.

4. Conclusions

HDI was successfully encapsulated in double-layered shells *via* optimizing the interfacial polymerization in an oil-in-water emulsion. The main conclusions can be drawn as follows:

• The optimal process determined is to emulsify the solution for 45 min and set the reaction at 50 °C for 2 h with 3 g Suprasec 2644.

• The shell tightness of microcapsules is improved significantly *via* the double-layered method. The initial evaporation temperature (148 °C) of the encapsulated HDI was much higher than that of pure HDI (117 °C), and the microcapsules had 1.6% weight loss compared with pure HDI with 90% weight loss after 1 h isothermal treatment at 100 °C. In addition, the double-layered shell showed excellent resistance to weakly and non-polar solvents even after 30 days immersion.

• Both fresh and hexane-treated microcapsule-modified epoxy coatings demonstrate outstanding anticorrosion performance *via* self-healing functionality of the released HDI in scratched areas during an accelerated corrosion process.

The robust microcapsules have great potential for practical applications in industrial coating and paint systems.

Acknowledgements

The authors appreciate the financial support from the Ministry of Education of Singapore (Grant # RG15/13). We very much appreciate the free Suprasec 2644 supplied by Huntsman Taiwan.

References

1 G. T. Bayer and M. Zamanzadeh, published internally by Matco Associates Sur. Fac. Epre. Pa. R. At. Ionandc. Oat. Ingappli. Cat. Ionpr. Ac. Tices., 2004, 331.
2 A. B. W. Brochu, S. L. Craig and W. M. Reichert, *J. Biomed. Mater. Res., Part A*, 2011, **96**, 492–506.

3 M. Wu, B. Johannesson and M. Geiker, *Construct. Build. Mater.*, 2012, **28**, 571–583.
4 A. Stankiewicz, I. Szczygiel and B. Szczygiel, *J. Mater. Sci.*, 2013, **48**, 8041–8051.
5 D. G. Shchukin, *Polym. Chem.*, 2013, **4**, 4871–4877.
6 H. Zhang and J. Yang, *J. Mater. Chem. A*, 2013, **1**, 12715–12720.
7 S. R. White, N. R. Sottos, P. H. Geubelle, J. S. Moore, M. R. Kessler, S. R. Sriram, E. N. Brown and S. Viswanathan, *Nature*, 2001, **409**, 794–797.
8 S. H. Cho, H. M. Andersson, S. R. White, N. R. Sottos and P. V. Braun, *Adv. Mater.*, 2006, **18**, 997–1000.
9 M. W. Keller, S. R. White and N. R. Sottos, *Adv. Funct. Mater.*, 2007, **17**, 2399–2404.
10 S. H. Cho, S. R. White and P. V. Braun, *Adv. Mater.*, 2009, **21**, 645–649.
11 M. D. Hager, P. Greil, C. Leyens, S. van der Zwaag and U. S. Schubert, *Adv. Mater.*, 2010, **22**, 5424–5430.
12 H. Zhang, P. Wang and J. Yang, *Compos. Sci. Technol.*, 2014, **94**, 23–29.
13 J. W. C. Pang and I. P. Bond, *Compos. Sci. Technol.*, 2005, **65**, 1791–1799.
14 R. Trask and I. Bond, *Smart Mater. Struct.*, 2006, **15**, 704.
15 R. Trask, G. Williams and I. Bond, *J. R. Soc., Interface*, 2007, **4**, 363–371.
16 K. S. Toohey, N. R. Sottos, J. A. Lewis, J. S. Moore and S. R. White, *Nat. Mater.*, 2007, **6**, 581–585.
17 G. O. Wilson, J. S. Moore, S. R. White, N. R. Sottos and H. M. Andersson, *Adv. Funct. Mater.*, 2008, **18**, 44–52.
18 K. S. Toohey, C. J. Hansen, J. A. Lewis, S. R. White and N. R. Sottos, *Adv. Funct. Mater.*, 2009, **19**, 1399–1405.
19 S. K. Ghosh, *Self-healing materials: fundamentals, design strategies, and applications*, John Wiley & Sons, 2009.
20 X. Chen, M. A. Dam, K. Ono, A. Mal, H. Shen, S. R. Nutt, K. Sheran and F. Wudl, *Science*, 2002, **295**, 1698–1702.
21 P. Cordier, F. Tournilhac, C. Soulié-Ziakovic and L. Leibler, *Nature*, 2008, **451**, 977–980.
22 S. M. Bleay, C. B. Loader, V. J. Hawyes, L. Humberstone and P. T. Curtis, *Composites, Part A*, 2001, **32**, 1767–1776.
23 E. B. Murphy, E. Bolanos, C. Schaffner-Hamann, F. Wudl, S. R. Nutt and M. L. Auad, *Macromolecules*, 2008, **41**, 5203–5209.
24 E. N. Brown, M. R. Kessler, N. R. Sottos and S. R. White, *J. Microencapsulation*, 2003, **20**, 719–730.
25 B. Blaiszik, M. Caruso, D. McIlroy, J. Moore, S. White and N. Sottos, *Polymer*, 2009, **50**, 990–997.
26 L. Yuan, G. Liang, J. Xie, L. Li and J. Guo, *Polymer*, 2006, **47**, 5338–5349.
27 J. Yang, M. W. Keller, J. S. Moore, S. R. White and N. R. Sottos, *Macromolecules*, 2008, **41**, 9650–9655.
28 M. Huang and J. Yang, *J. Mater. Chem.*, 2011, **21**, 11123–11130.
29 M. Huang and J. Yang, *Prog. Org. Coat.*, 2014, **77**, 168–175.
30 M. Huang, PhD thesis, Nanyang technological university, 2013.
31 C. J. Fan and X. D. Zhou, *Polym. Adv. Technol.*, 2009, **20**, 934–939.
32 P. D. Tatiya, R. K. Hedaoo, P. P. Mahulikar and V. V. Gite, *Ind. Eng. Chem. Res.*, 2013, **52**, 1562–1570.
33 L. Yuan, G.-Z. Liang, J.-Q. Xie, L. Li and J. Guo, *J. Mater. Sci.*, 2007, **42**, 4390–4397.
34 G. Wu, J. L. An, D. W. Sun, X. Z. Tang, Y. Xiang and J. L. Yang, *J. Mater. Chem. A*, 2014, **2**, 11614–11620.
35 G. Wu, J. An, X.-Z. Tang, Y. Xiang and J. Yang, *Adv. Funct. Mater.*, 2014, **24**, 6751–6761.
36 W. E. Brown, A. H. Green, T. E. Cedel and J. Cairns, *Environ. Health Perspect.*, 1987, **72**, 5–11.
37 D. J. Buckley, M. Berger and D. Poller, *J. Polym. Sci.*, 1962, **56**, 163–174.
38 B. Yang, W. Huang, C. Li and L. Li, *Polymer*, 2006, **47**, 1348–1356.
39 R. Pearson and E. Williams, *J. Polym. Sci., Polym. Chem. Ed.*, 1985, **23**, 9–18.
40 P. W. Morgan and S. L. Kwolek, *J. Polym. Sci.*, 1959, **40**, 299–327.
41 C. s. Schollen and F. D. Stewart, *Angew. Makromol. Chem.*, 1973, **29–3**, 413–430.
42 E. B. G. William De Santis, *US Pat.* 3,779,794, N.J, 1973.
43 M. Salame and S. Steingiser, *Polym.–Plast. Technol. Eng.*, 1977, **8**, 155–175.
44 P. J. Flory and J. Rehner Jr, *J. Chem. Phys.*, 1943, **11**, 521–526.
45 T. Canal and N. A. Peppas, *J. Biomed. Mater. Res., Part A*, 1989, **23**, 1183–1193.
46 A. Jonquières, D. Roizard and P. Lochon, *J. Appl. Polym. Sci.*, 1994, **54**, 1673–1684.
47 N. Schneider, J. Illinger and M. Cleaves, *Polym. Eng. Sci.*, 1986, **26**, 1547–1551.
48 N. A. Peppas and S. R. Lustig, *Ann. N. Y. Acad. Sci.*, 1985, **446**, 26–40.
49 M. Szycher, *Szycher's handbook of polyurethanes*, CRC Press, 2012.
50 Huntsman, A guide to thermoplastic polyurethanes (TPU).
51 D. A. P. Rebecca and A. Bader, *Engineering Polymer Systems for Improved Drug Delivery*, Wiley, 2014.
52 N. M. Lamba, K. A. Woodhouse and S. L. Cooper, *Polyurethanes in biomedical applications*, CRC press, 1997.